

White-Light-Emitting Diodes with Quantum Dot Color Converters for Display Backlights

By Eunjoo Jang,* Shinae Jun, Hyosook Jang, Jungeun Lim, Byungki Kim, and Younghwan Kim

Quantum dots (QDs) have shown great potential for next-generation displays owing to their color tunability, narrow emission, and high luminescence efficiency. However, it is difficult to maintain the initial optical properties of the QDs to be maintained during device fabrication and long-term operation. We report here new structures of multiply passivated QDs that show almost 100% quantum efficiency (QE) and high stability in a solid-state devices. The green- and red-light-emitting QDs were used as color converters in InGaN blue LEDs to achieve up to 72% and 34% external quantum efficiencies (EQEs), respectively, and their initial EQEs were maintained for 2200 h. The extremely cool-white QD-LEDs were prepared for a display backlight, and they showed 41 lm W⁻¹ at 100,000K color temperature and more than 100% color reproducibility compared to the National Television Systems Committee (NTSC) standard in the Commission internationale de l'éclairage (CIE) 1931 color space. Using the white QD-LED backlight, a 46 inch LCD panel was successfully demonstrated for the first time.

QDs have been highlighted in nanotechnology owing to their novel optoelectronic properties resulting from the size quantization effect. Decades of effort have led to the preparation of QDs with controllable energy bandgaps, high QE, exquisite color purity, extended lifetime, and multifunctionality.^[1–9] Once QDs acquire the aforementioned characteristics, they can be utilized in many potential applications, especially for display devices: Hybrid LEDs, which employ QDs as active electroluminescent materials working through direct electron–hole injection, have attracted considerable attention,^[10–13] and color-converting LEDs, which use inorganic InGaN LEDs with QDs as color converters, have appeared extensively in recent reports.^[7,14–18]

Currently, white LEDs are attracting a great deal of attention and their commercialization is expanding to high-volume applications, including general lighting and displays. Especially, white LED backlights for liquid-crystal displays (LCDs) have many advantages compared to the prevailing fluorescent lamp backlights in terms of high efficiency and the slim size of packages. However, white LED backlights need to be more cost-effective and more color-saturated. At present, there are several combinations for obtaining white LEDs. The mixed light from a

blue InGaN LED with a yellow phosphor (cerium-doped yttrium aluminum garnet: YAG) makes a cool white LED. This is the most efficient and economical structure, but the pale white light from blue and yellow hues cannot express the natural colors of objects faithfully in general circumstances.^[19] The red, green, and blue (RGB) three primary color InGaN LEDs make white light with excellent color gamut. However, the efficiency of green LEDs is still low, and the separate driving circuits for each RGB LED lead to higher costs than for single-chip white LEDs. White LEDs consisting of a blue LED with RG phosphors produce a better color gamut than the blue LED and YAG phosphor. However, to date, few red phosphors that can be excited by low energy wavelengths (blue light) are available, and on top of that, the phosphors exhibit low efficiencies and broad emissions.^[20] There have been many efforts to develop QD color converters for LEDs for general purposes after Bawendi's report on QD–polymer composites.^[21] The RG QDs on a blue LED showed much improved color rendering index (CRI) up to 91 at CIE 1931 coordinate (0.33, 0.33).^[22] It was further attempted to use red QDs with a green phosphor to enhance the efficacy up to 14 lm W⁻¹ while maintaining CRI value around 90 at CIE 1931.^[14] Also, it was reported that silica-coated InP/ZnS QDs together with a green phosphor and YAG showed an efficacy of 15 lm W⁻¹ and CRI value up to 86 at 3900 K.^[15] The white QD-LEDs reported to date exhibited improved CRI values by having spectra designed to extend broadly over all visible wavelengths.^[16–18] However, unlike general lighting applications, display backlights employ RGB color filters to reproduce color images through the combination of the RGB primary colors. The wavelengths not transmitted by the color filter would cause the energy loss. It is necessary to optimize the combination of highly defined RGB colors with narrow emissions for white backlights. Therefore, QDs with narrow emission at controllable wavelengths have great advantages compared to conventional phosphors. However, the previous QD-LEDs showed only 7 lm W⁻¹ efficacy, and the peak emissions of red and green lights were not optimized for displays.^[22] The low efficacy of QD-LEDs would result in initial low QEs for the QDs as well as the decrease of QE during processing for device fabrication.

In this Communication, we report highly luminescent, multishell QDs showing almost unit of QE, and white QD-LEDs showing 41 lm W⁻¹ efficacy at the coordinate (x, y) = (0.24, 0.21) in CIE 1931 and 100% color reproducibility compared to NTSC color space.^[19] After Hines and Guyot-Sionnest published reports of ZnS-capped CdSe QDs showing luminescence up to 50% QE,^[1] considerable efforts were devoted to optimizing QD structures to achieve intense and narrow emissions.^[2–7] However, their luminescence efficiencies were easily degraded

[*] Dr. E. Jang, Dr. S. Jun, Dr. H. Jang, J. Lim, Dr. B. Kim, Dr. Y. Kim
Materials Research Center
Samsung Advanced Institute of Technology
Samsung Electronics, Mt. 14-1, Nongseo-Dong
Giheung-Gu, Yongin-Si, Gyeonggi-Do, 449-712 (Republic of Korea)
E-mail: ejjang12@samsung.com

DOI: 10.1002/adma.201000525

during the processes of ligand exchange,^[23] incorporation into solid states, and long-term exposure to photoexcitation.^[24,25] This is due to the surface traps generated by the detachment of organic passivating ligands, destabilized core/shell interfaces, or the structural changes to oxides. Although the QEs of red-light-emitting QDs were known to be 80–90%, the QE and stability of green QDs are far from satisfactory. The purchased CdSe/ZnS (Evident Technology) core/shell QDs routinely showed 50% QE at 530 nm emission. Recently, it was reported that the extremely small CdSe/CdS core/shell QDs (ca. 2.8 nm) showed 60% QE at 517 nm emission,^[26] and CdZnSe/CdZnS alloy core/shell QDs (ca. 3 nm) showed 50–60% QE at 520 nm.^[6] The stabilities of these small QDs have never been reported in detail. Such small QDs are more difficult to passivate uniformly with a thick shell without causing distortion of the crystalline lattice. To make relatively large QDs for green emission, we chose blue-light-emitting interfused alloy CdSe//ZnS QDs^[5] as cores, and passivated them with a gradient multilayered CdSZnS shell that induces red-shifted emission and surface passivation.^[27,28] The growth of the CdSZnS multishell was carried out in a single batch by utilizing the difference of the reaction rates of Cd and Zn with S; the elemental composition gradually changed from CdS to ZnS, which reduced lattice mismatch effectively.^[27] The detailed method of synthesis is given in the Supporting Information (S1). **Figure 1** shows diagrams of green-light-emitting QD structures and their absorption and emission spectra. The CdSe core was prepared to give the first absorption maximum at 465 nm and the emission maximum at 490 nm. Then the first ZnS shell was grown on the CdSe core and interfused into the core to produce CdSe//ZnS alloy QDs. The first absorption and the emission maxima for the CdSe//ZnS alloy moved to 435 nm and 469 nm, respectively. The degree of blue shift during the first ZnS coating could be controlled by changing the ratio of the CdSe core and the ZnS precursor concentrations. On the blue CdSe//ZnS QDs, CdSZnS was coated to make CdSe//ZnS/CdSZnS QDs, which showed red-shifted absorption and emission at 486 nm and 530 nm, respectively. The degree of red shift during the second CdSZnS coating could be controlled by changing the amount of Cd and Zn precursors. Transmission electron microscopy (TEM) images show that the size of the CdSe//ZnS alloy increased from $d = 3 \text{ nm} \pm 0.3 \text{ nm}$ (CdSe core) to $d = 4.5 \text{ nm} \pm 0.5 \text{ nm}$, and the size of CdSe//ZnS/CdSZnS increased further to $d = 5.5 \text{ nm} \pm 0.5 \text{ nm}$. Elemental analysis by inductively coupled plasma atomic emission spectroscopy (ICP-AES; see Supporting Information, S2) showed that the molar ratio of Zn and S in the CdSe//ZnS alloy to Se increased, compared with the CdSe core, to 4.7 and 3.3, respectively. Also, the molar ratio of Zn and S in CdSe//ZnS/CdSZnS to Se increased to 15.3 and 19, respectively. The elemental composition of the CdSe core showed an unbalanced ratio of 1.5/1 for Cd/Se. This could result from the excess metal–surfactant complexes that existed on the nanoparticle surface. After the ZnS coating and the interfusion reaction to prepare CdSe//ZnS, the ratio of Cd to Se decreased to 1.3 because some excess complexes were removed. On the basis of the size of the CdSe//ZnS, the increment of Cd and Zn, and the atomic lattices of CdS and ZnS, it could be estimated that the CdSe//ZnS/CdSZnS had two monolayers of CdS and three monolayers of

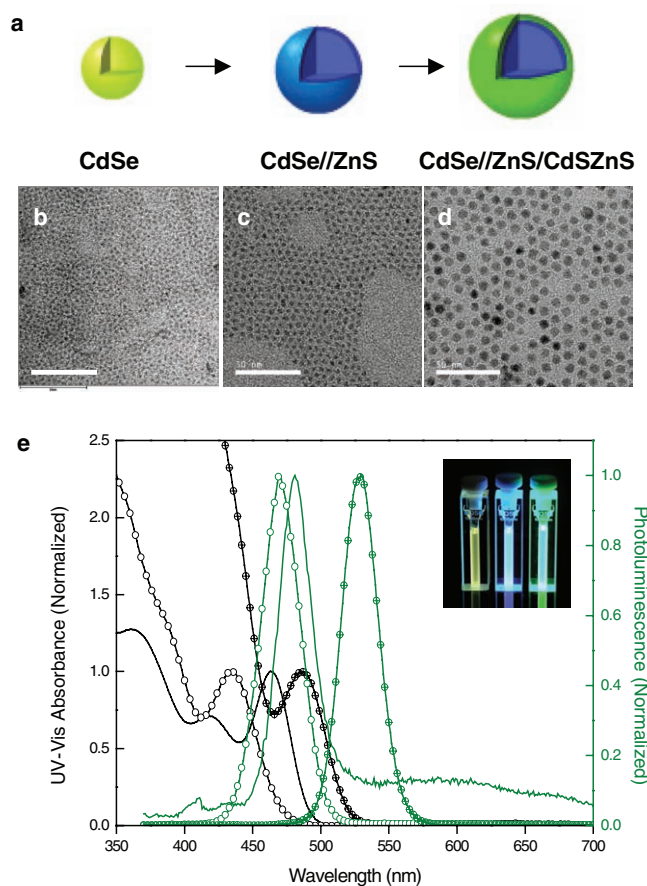
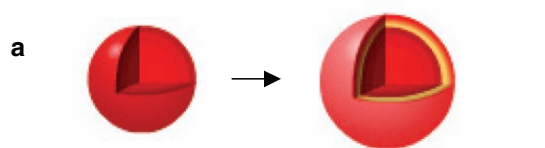


Figure 1. a) Schematic structures of the growth of green QDs. b–d) TEM images of CdSe core (b), CdSe//ZnS alloy (c), and CdSe//ZnS/CdSZnS QDs (d). Each scale bar represents 50 nm. e) Absorption (black) and emission (green) spectra of CdSe core (solid line), CdSe//ZnS (circles), and CdSe//ZnS/CdSZnS (circled crosses). Inset: QD solutions under 365 nm UV light.

ZnS on the CdSe//ZnS if the layers formed separately. These large green QDs with multilayers showed 100% QE compared to the Coumarin 540 reference,^[29] and a full width at half maximum (FWHM) of 28 nm.

Highly luminescent red-light-emitting QDs, CdSe/CdS/ZnS/CdSZnS, were also prepared by adding a CdSZnS coating to the previously reported CdSe/CdS/ZnS.^[7] For the CdSe/CdS/ZnS QDs, the CdS inner shell causes a bandgap shift to longer wavelengths as well as QE improvement, and the ZnS outer shell results in mainly QE improvement. In order to synthesize QDs with thicker final shell for better stability, a CdZnS layer was grown on the ZnS layer additionally because the CdZnS layer could alleviate the lattice strain of ZnS on CdSe/CdS. **Figure 2** shows diagrams of the structures together with TEM images and absorption and emission spectra. The additional CdSZnS coating on the CdSe/CdS/ZnS moved the emission maximum from 599 nm to 630 nm while maintaining the FWHM of 35 nm. The inset shows both CdSe/CdS/ZnS and CdSe/CdS/ZnS/CdSZnS QDs in toluene. Both of them glow very strongly, even under normal daylight, but the additionally coated one shows brighter glinting. The QEs were improved after the



CdSe/CdS/ZnS CdSe/CdS/ZnS/CdSZnS

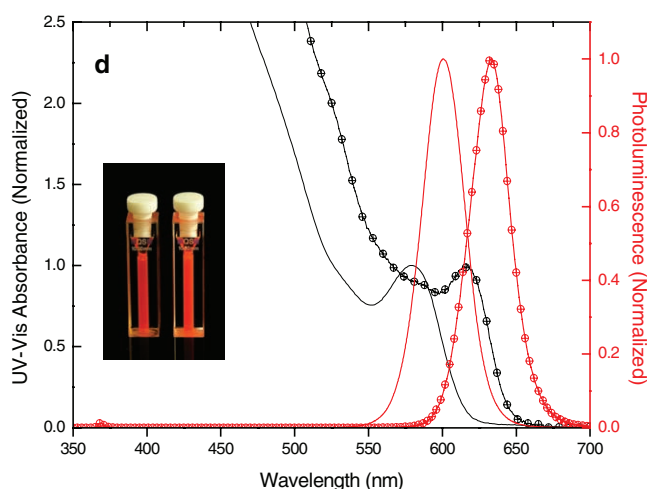
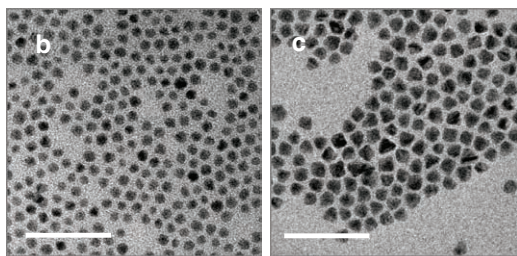


Figure 2. a) Schematic structures for the growth of red QDs. b,c) TEM images of CdSe/CdS/ZnS (b) and CdSe/CdS/ZnS/CdSZnS (c). Each scale bar represents 50 nm. d) Absorption (black) and emission (red) spectra of CdSe/CdS/ZnS (solid line) and CdSe/CdS/ZnS/CdSZnS (circled crosses). Inset: QD solutions under daylight.

additional CdSZnS coating from 75% to 95% in reference to Rhodamin 6G.^[29] The TEM images clearly show that the particle size increased from $d = 6.8 \text{ nm} \pm 0.3 \text{ nm}$ to $d = 8.6 \text{ nm} \pm 0.3 \text{ nm}$ while uniform size and shape were retained.

The EQEs of the CdSe//ZnS/CdSZnS green QDs and CdSe/CdS/ZnS/CdSZnS red QDs in LEDs were measured at different concentrations of QDs in silicone encapsulant. (Figure 3) The preparation method of the QD-LEDs is described in the Supporting Information (S1). The EQEs of green QDs in LEDs were 52%, 56%, 59%, and 72% at optical densities^[30] of 0.07, 0.05, 0.035, and 0.017, respectively, and those of red ones were 23%, 24%, and 34% at optical densities of 0.014, 0.007, and 0.0035, respectively. The peak wavelengths and FWHMs of the green and red QDs in LEDs were maintained. Although these QD-LEDs showed quite high efficiencies at optimized wavelengths, they still did not provide the same level of light-emitting efficiencies as the QD solutions. The efficiencies could have been reduced during the packaging process, in which surface defects

of QDs were generated through the loss of coordinating ligands or different side reactions with various components in the silicone encapsulants at high temperatures above 150 °C. Also, the significantly aggregated QDs in silicone encapsulant could cause re-absorption and scattering, which would lead to a decrease in efficiency depending on the concentration. A few approaches have been suggested to disperse QDs in silicone polymers uniformly by ligand exchange, the modification of silicone structures, and the addition of ambi-compatible dispersants,^[31] however, not much success has been achieved so far. Therefore, the EQEs of QD-LEDs would be much enhanced and concentration-independent when the dispersion of QDs in silicones were to be improved. A study of the dispersion of nanoparticles is currently in progress. The changes of EQEs of the red and green QD-LEDs were monitored while they were operated at 20 mA, 3 V, under ambient conditions without any heat sink. The concentrations of QDs were selected to be similar to those in white QD-LEDs (optical density 0.035 for green and 0.0035 for red). The efficiencies of the QD-LEDs were maintained for 2200 h, and the peak wavelengths were also maintained. Extrapolation indicates that half-lifetime could be longer than 15000 h, which is the timespan that mobile displays usually guarantee.

The color coordinate of the white QD-LED was optimized at (0.24, 0.21) in CIE 1931 for LCD backlight. The red and green QDs at the controlled concentrations (optical density 0.035 at 486 nm for green and 0.0035 at 516 nm for red)^[32] were mixed with silicones and dispersed on a blue LED. Also, as a comparison, a white phosphor LED with the same color coordinate was prepared with a Eu-doped CaAlSiN₃ red phosphor^[33] (peak at 650 nm, FWHM = 94 nm, see Supporting Information S3), and a Eu-doped β -SiAlON green phosphor^[34] (peak at 537 nm, FWHM = 56 nm, see Supporting Information S3). Figure 4a shows the spectra of both white LEDs' light intensities (solid line) and their luminous fluxes (hatched areas). Although the phosphor-LED emitted more radiation than the QD-LED over most of the wavelengths, the luminous efficacies of both LEDs were very similar: 41 lm W⁻¹ for the QD-LED and 40 lm W⁻¹ for the phosphor-LED. The reason for the disparity between the light intensity and the efficacy is due to the photopic sensitivity of the human eye. A considerable portion of the radiation from the blue LED and the red phosphor could not contribute to the luminous efficacy. Therefore, the luminous fluxes for both QD-LEDs and phosphor-LEDs were similar, and this agrees well with the luminous efficacies both LEDs. The peak of the phosphor-LED's luminous flux spectrum in the red region appeared at 594 nm, which resulted from the overlap of the green and red phosphors' broad emissions. However, the peak of the QD-LED's luminous flux almost maintained its original wavelength at 625 nm. Therefore, the QD-LED could represent a more vivid red color than the phosphor-LED. The color gamut for each white LED was measured with a PR-705 SpectraScan (Photo Research Inc.); the RGB color coordinates for the QD-LED and the phosphor-LED were (0.67,0.31), (0.19,0.71), (0.15,0.06) and (0.66,0.32), (0.28,0.65), (0.15,0.05), respectively. The area of the RGB triangle of the white QD-LED covered most of the NTSC color space (104.3%), but the phosphor-LED covered only 85.6% (Figure 4a, inset). A LED backlight was fabricated with 960 white QD-LEDs, and a 46 inch

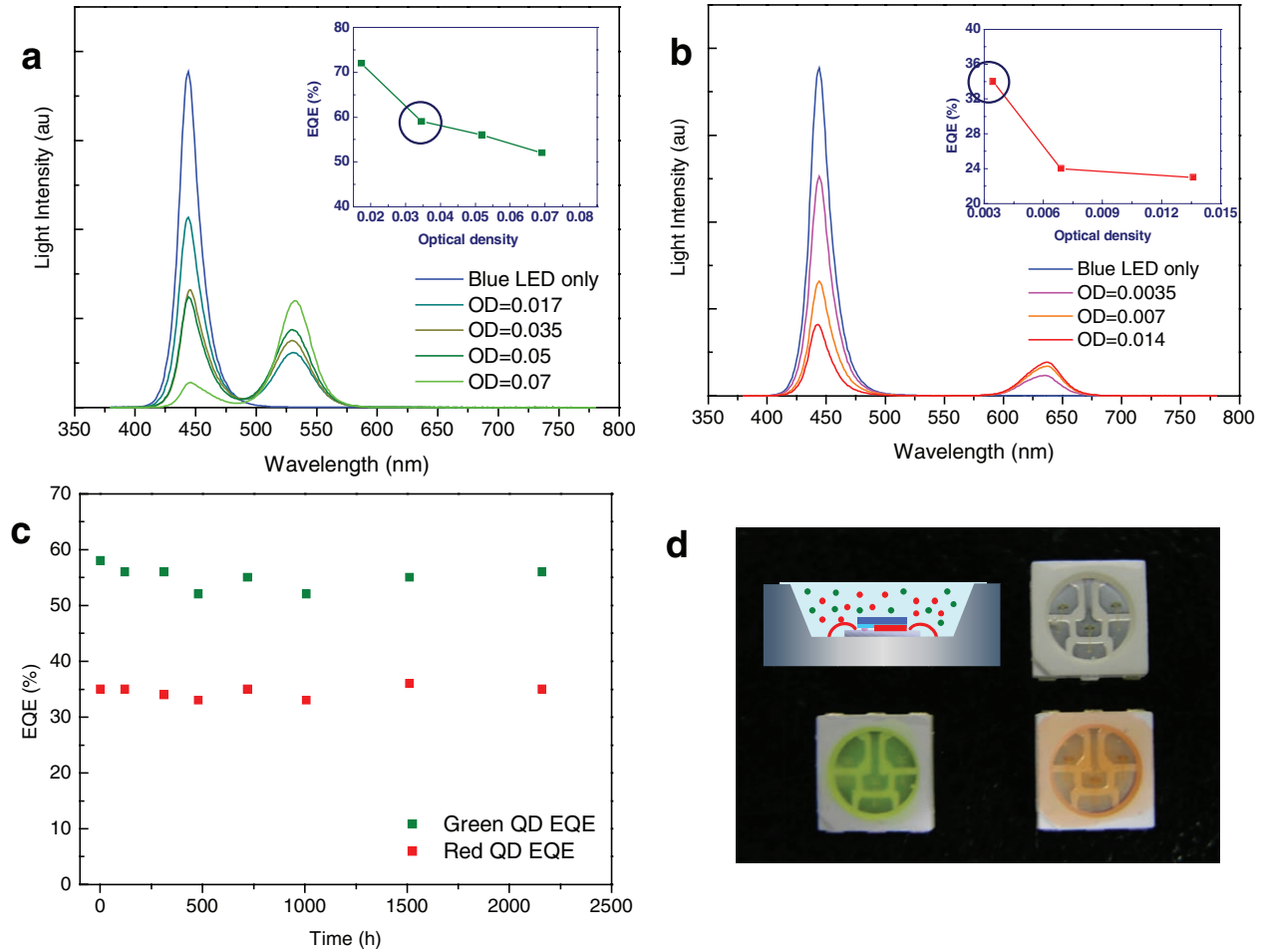


Figure 3. a) Spectra of the green QD-LEDs with various QD concentrations. Inset: EQEs of the QDs in the LED according to the QD concentrations. b) The same as (a) except for red QD-LEDs. c) EQEs of the QD-LEDs over long-term operation. The concentration of each QD is indicated by the circled points in the insets of (a) and (b). d) Schematic diagram of QD LED, side view (upper left); blue LED package (upper right); green QDs (lower left) and red QDs with silicone resin dispersed and cured (lower right). Photo was taken under normal daylight.

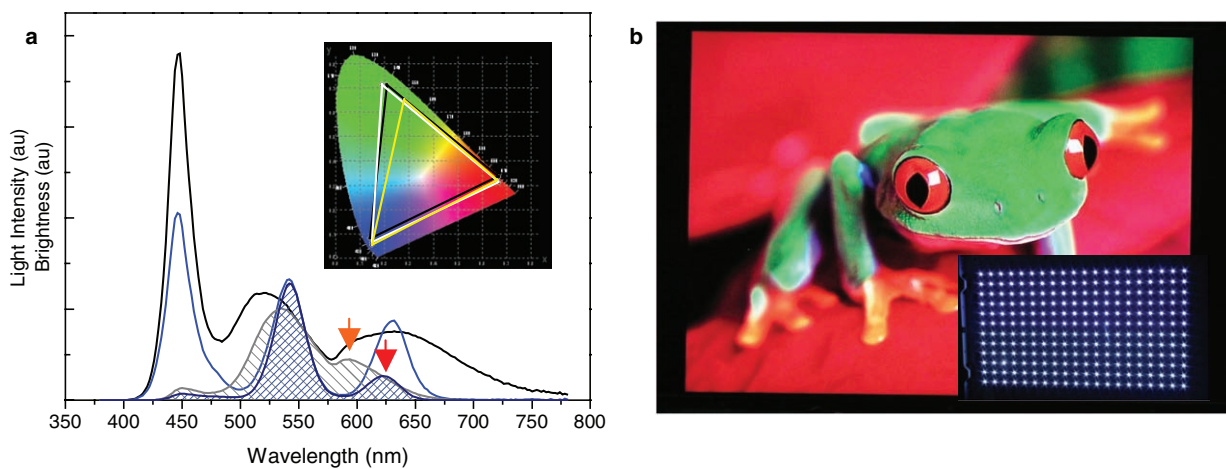


Figure 4. a) Light intensity spectra (solid line) and brightness (hatched area) of the QD-LED (blue) and the phosphor-LED (grey). Inset: Color triangles of the QD-LED (white) and the phosphor-LED (yellow) compared to NTSC1931 (black). b) Display image of a 46 inch LCD TV panel and a quarter of the white QD-LED backlights (inset).

LCD TV panel was successfully demonstrated for the first time (Figure 4b). This result takes us one step closer toward developing QDs specially tailored for high performance display applications.

In summary, we have described detailed synthetic methods for the highly luminescent, multishell-structured green CdSe//ZnS/CdSZnS QDs and red CdSe/CdS/ZnS/CdSZnS QDs, which showed up to 100% QEs. The QDs were packaged as green and red color converters in blue LEDs to prepare white LEDs for display backlights. The EQEs of QDs in the LEDs were dependent on the QD concentration in the silicone composites. The EQEs of green and red QD-LEDs reached up to 72% and 34% respectively, and the QD-LED maintained their initial efficiency for longer than 2200 hours under ambient conditions. The white QD-LED adjusted at the color coordinate of (0.24, 0.21) in CIE 1931 for backlight application showed luminous efficacy of 41 lm W⁻¹ and color reproducibility of 100% compared to the NTSC color space. Also, the white QD-LED backlight was successfully integrated in a 46 inch LCD TV panel to demonstrate excellent color gamut.

Supporting Information

Supporting Information is available online from WileyInterscience or from the authors.

Acknowledgements

The authors thank J. Park and J. Byun at Samsung Electronics for the fabrication of the 46 inch LCD TV panels.

Received: February 10, 2010

Revised: March 24, 2010

Published online: May 31, 2010

- [1] M. A. Hines, P. Guyot-Sionnest, *J. Phys. Chem.* **1996**, *100*, 468.
- [2] X. Peng, M. C. Schlamp, A. V. Kadavanich, A. P. Alivisatos, *J. Am. Chem. Soc.* **1997**, *119*, 7019.
- [3] B. O. Dabbousi, J. Rodriguez-Viejo, F. V. Mikulec, J. R. Heine, H. Mattoussi, R. Ober, K. F. Jensen, M. G. Bawendi, *J. Phys. Chem. B* **1997**, *101*, 9463.
- [4] J. S. Steckel, J. P. Zimmer, S. Coe-Sullivan, N. E. Stott, V. Bulovic, M. G. Bawendi, *Angew. Chem. Int. Ed.* **2004**, *43*, 2154.
- [5] S. Jun, E. Jang, *Chem. Commun.* **2005**, 4616.
- [6] J. S. Steckel, P. Snee, S. Coe-Sullivan, J. P. Zimmer, J. E. Halpert, P. Anikeeva, L.-A. Kim, V. Bulovic, M. G. Bawendi, *Angew. Chem. Int. Ed.* **2006**, *45*, 5796.
- [7] J. Lim, S. Jun, E. Jang, H. Baik, H. Kim, J. Cho, *Adv. Mater.* **2007**, *19*, 1927.
- [8] S. Haubold, M. Haase, A. Kornowski, H. Weller, *ChemPhysChem* **2001**, *2*, 331.
- [9] R. Xie, D. Battaglia, X. Peng, *J. Am. Chem. Soc.* **2007**, *129*, 15432.
- [10] J. Lee, V. C. Sundar, J. R. Heine, M. G. Bawendi, K. F. Jensen, *Adv. Mater.* **2000**, *12*, 1102.
- [11] S. Coe, W. K. Woo, M. Bawendi, V. Bulovic, *Nature* **2002**, *420*, 800.
- [12] P. O. Anikeeva, J. E. Halpert, M. G. Bawendi, V. Bulovic, *Nano Lett.* **2009**, *9*, 2532.
- [13] K.-S. Cho, E. K. Lee, W.-J. Joo, E. Jang, T.-H. Kim, S. J. Lee, S.-J. Kwon, J. Y. Han, B.-K. Kim, B. L. Choi, J. M. Kim, *Nat. Photon.* **2009**, *3*, 341.
- [14] H. S. Jang, H. Yang, S. W. Kim, J. Y. Han, S.-G. Lee, D. Y. Jeon, *Adv. Mater.* **2008**, *20*, 2696.
- [15] J. Ziegler, S. Xu, E. Kucur, F. Meister, M. Batenschuk, F. Gindele, T. Nann, *Adv. Mater.* **2008**, *20*, 4068.
- [16] M. Ali, S. Chattopadhyay, A. Nag, A. Kumar, S. Sapra, S. Chakraborty, D. D. Sarma, *Nanotechnology* **2007**, *18*, 075401.
- [17] S. Nizamoglu, T. Ozel, E. Sari, H. V. Demir, *Nanotechnology* **2007**, *18*, 065709.
- [18] S. Nizamoglu, G. Zengin, H. V. Demir, *Appl. Phys. Lett.* **2008**, *92*, 031102.
- [19] R. S. Berns, *Billmeyer and Saltzman's Principles of Color Technology*, 3rd ed., Wiley, New York **2000**.
- [20] S. Neeraj, N. Kijima, A. K. Cheetham, *Chem. Phys. Lett.* **2004**, *387*, 2.
- [21] J. Lee, V. C. Sundar, J. R. Heine, M. G. Bawendi, K. F. Jensen, *Adv. Mater.* **2000**, *12*, 1102.
- [22] H. Chen, C. Hsu, H. Hong, *IEEE Photon. Technol. Lett.* **2006**, *18*, 193.
- [23] S. Jeong, M. Achermann, J. Nanda, S. Ivanov, V. I. Klimov, J. A. Hollingsworth, *J. Am. Chem. Soc.* **2005**, *127*, 10126.
- [24] A. Y. Nazzal, X. Wang, L. Qu, W. Yu, Y. Wang, X. Peng, M. Xiao, *J. Phys. Chem. B* **2004**, *108*, 5507.
- [25] D. V. Talapin, I. Mekis, S. Götzinger, A. Kornowski, O. Benson, H. Weller, *J. Phys. Chem. B* **2004**, *108*, 18826.
- [26] D. Pan, Q. Wang, S. Jiang, X. Ji, L. An, *Adv. Mater.* **2005**, *17*, 176.
- [27] S. Jun, E. Jang, J. Lim, *Nanotechnology* **2006**, *17*, 3892.
- [28] L. Manna, E. C. Scher, L.-S. Li, A. P. Alivisatos, *J. Am. Chem. Soc.* **2002**, *124*, 7136.
- [29] L. Qu, X. Peng, *J. Am. Chem. Soc.* **2002**, *124*, 2049.
- [30] Optical density is the absorbance of 1 vol% diluted QD solution in reference solvent at the first absorption maximum.
- [31] J. W. Parce, J. Chen, B. Dubrow, B. Freeman, E. C. Scher, J. A. Whiteford, *US patent*, 7374807.
- [32] W. W. Yu, L. Qu, W. Guo, X. Peng, *Chem. Mater.* **2003**, *15*, 2854.
- [33] M. Mikami, K. Uheda, N. Kijima, *Phys. Status Solidi A* **2006**, *203*, 2705.
- [34] J. H. Ryu, H. S. Won, H. Suzuki, S. H. Kim, C. Yoon, *J. Ceram. Soc. Jpn.* **2008**, *116*, 389.